Comparison of fracture toughness values of normal and high strength concrete determined by three point bend and modified disk-shaped compact tension specimens

Stanislav Seitl
Academy of Sciences of the Czech Republic, Institute of Physics of Materials, v. v. i., Žižkova 22, 616 62 Brno, Czech Republic
seitl@ipm.cz, http://orcid.org/0000-0002-4953-4324

José D. Ríos, Hector Cifuentes
Grupo de Estructuras, ETSI, Universidad de Sevilla, Camino de los descubrimientos s/n, 41092 Sevilla, Spain.
jdrios@us.es,
bulte@us.es, http://orcid.org/0000-0001-6302-418X

ABSTRACT. The modified disk shaped compact tension test is a configuration derived from standard compact tension test that is used for measuring fracture mechanical properties of primarily metallic materials. The compact tension configuration is commonly used for measurement fracture mechanical properties as e.g. fracture toughness, Young's modulus, work of fracture etc. The modified compact tension tests imply significant modifications of the specimen morphology in order to avoid premature failure. The modified compact tension test is not proper for quasi-brittle materials due to its complicated shape (steel-concrete interface), but it is easily extracted from drill core and we do not need large amount of material for obtaining fracture properties as we need for e.g. three- or four- point bend test. Since it is a new test method, a wide range of tests is needed to be done before it can be applied. In the paper the selected outputs of the experiments performed on normal and high strength concrete will be processed and the values of fracture mechanical parameters will be discussed.

KEYWORDS. Concrete; Stress intensity factor; T-stress; Compact tension test; Fracture behavior; Fracture mechanics; Constraint.

Citation: Seitl, S., Ríos, J.D., Cifuentes, H. Comparison of fracture toughness values of normal and high strength concrete determined by three point bend and modified disk-shaped compact tension specimens, Frattura ed Integrità Strutturale, 42 (2017) 56-65.

Received: 31.05.2017
Accepted: 08.06.2017
Published: 01.10.2017

INTRODUCTION

The assessment of residual life of existing concrete structures has been an attractive topic for the researchers for decades. This could be carried out to regularly monitor the health of old/important concrete structures and/or to evaluate damaged concrete structures to conserve the structural integrity and for constructional issues i.e. repair and

modification. The importance of rehabilitating the concrete structures has become obvious especially in some regions of the world that have been suffering from e.g. earthquakes, flooding, military conflict, terrorist attacks etc. Repairing these structures instead of destroying and rebuilding them could save time and finance from the one side and save the nature (do not need preparation of new concrete etc.) from the other side. The structural assessment is carried out by evaluating the concrete quality indicate by e.g. compressive strength, fracture toughness, fracture energy, Young's modulus, tensile splitting strength, etc.

For evaluation of all fracture mechanical properties of materials like concrete, standardized methodology is not published yet. There are norms: ACI [1] and [8] for compressive strength, [9] for flexural strength of test specimens, tensile splitting strength [10], Young's modulus [7], recommendations for fracture energy determination for three-point-bend (TPB) specimen in RILEM [24] and for wedge splitting test (WST) specimen in [18] or tensile strength and fracture toughness [33]. In literature we can found that researchers used various geometries for measurement of concrete fracture properties , e.g. TPB [13,17], WST [4, 21], the combination of TPB and WST [29-30], disk shaped compact tension [14, 32] and another configurations can be found in handbooks e.g. [22, 28].

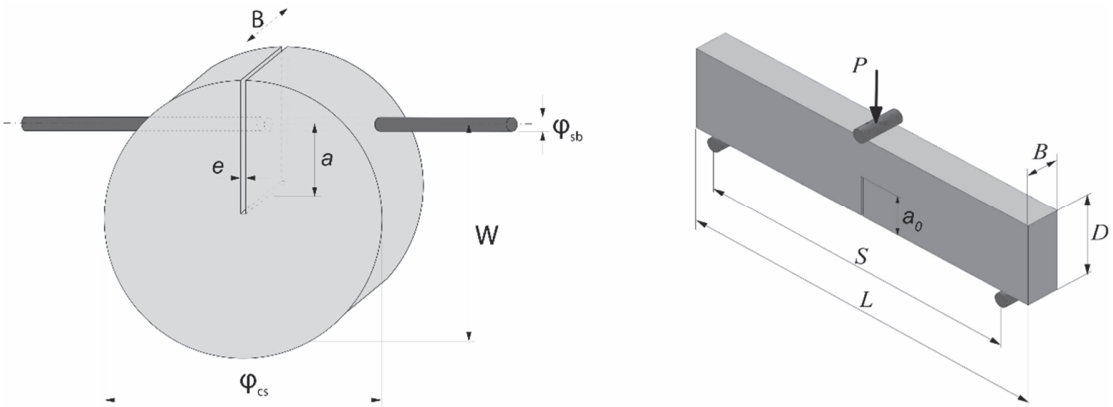

(a) (b)

Figure 1: Schemes of modified compact tension (a) and three-point bend test (b) with the characteristic dimensions

Widely used testing procedure for measuring the fracture properties of diverse types of materials is a compact tension (CT) test see in ASTM Standard E-399 [2], plastics (ASTM Standard D5045-14) or composite materials with limited orthotropy [23]. Nevertheless, tests applied to concrete samples have not attained satisfactory results leading to the failure prematurely. Wagoner et al. [32] carried out the CT test on concrete specimens and the premature failure was attained in 50% tested cases at the pulling load holes.

Modify compact tension (MCT) test is a different version of CT test to reliably obtain the fracture properties of quasi-brittle materials (like the concrete). The specimen morphology is adapted to avoid premature failures during testing procedure. The load holes are replaced for two longitudinal steel bars, inserted in the specimen during its casting stage, to avoid generation of local fracture at load holes, the geometry of MCT and TPB specimens are shown schematically in Fig. 1.a and b, respectively.

For fracture analysis of a test specimen, the major parameters that characterize the stress and strain fields around the crack tip should be known for the test specimen. As MCT test is a very recent methodology of calculus, detailed studies must be carried out to deepen on the reliability of the results. In this way, Seitl and Viszlay [26] provided calibration curves corresponding to four fracture mechanical parameters (stress intensity factor, K_I, T-stress, crack opening displacement, COD, and crack mouth opening displacement, CMOD) for cement based materials varying the elasticity modulus (E). So significant amount of evaluations is measured by means of finite element model of the MCT test developed for them. The results were determined from the aforementioned model for 2D and 3D simulations and discussed the obtained values.

In this paper, experimental measured data from tests performed by Cifuentes et al. [5, 6] to assess the use of MCT test for measuring the fracture energy (G_F) on normal-strength concrete (NSC) and high-strength concrete (HSC) will be processed and analyzed for various crack length to width ratios and the values of fracture mechanics parameters (K_I and T-stress) will be evaluated and discussed using the outputs-calibration curves- from previous performed numerical simulations. Afterwards, an assessment of all procedures used to calculate fracture parameters will be performed.

The rest of this paper is organized as follows. Details of experimental campaign, normal and high strength concrete mechanical properties and dosages are shown in Section 2. The numerical simulations and related calibration curves

accounted on this work to calculate fracture parameters, are presented in Section 3. The values of fracture parameters obtained through the empirical and numerical calibration curves are shown and discussed in Section 4. Finally, the conclusions of this work are given in Section 5.

EXPERIMENTAL CAMPAIGN

The experimental data used to obtain the two fracture parameters, K_I and T-stress, by means of calibration curves from numerical simulations, presented in next Section, were attained in a previous paper by Cifuentes et al. [5]. That paper was focused on the reliability of MCT test for measuring the fracture energy (G_F) on normal-strength (NSC) and high-strength concrete (HSC) comparing the results with those achieved from three-point bend (TPB) test. The fracture parameters will be calculated for the aforementioned normal strength concrete (NSC) and high strength concrete (HSC) whose constituents and mix proportions are shown in Tab. 1.

Constituents	NSC Content [kg/m³]	HSC Content [kg/m³]
Cement	376	500
Micro-silica	-	75
Coarse aggregate (crushed limestone) <10 mm	580	990
Sand < 2 mm	739	660
Limestone powder < 2 mm	192	134
Water	545	105
Super-plasticizer	3.0	18.4
Flow spread (mm)	710	695
T_{500} (s)	3.1	3.4

Table 1: Constituents and mix proportions for NSC and HSC.

The specimen geometry for MCT and TPB test are listed in Tab. 2. Three different types of MCT specimens were casted. From MCT1 to MCT3, the distance from the load axis to the backside of the specimen, W, measures 112.5 mm. For each type, specimens with three different relative notch length, α, (0.1, 0.3 and 0.5) were tested. Regarding TPB test, two type of specimens were accounted with a relative notch length, α, of 0.05 and 0.5. All specimens were manufactured for NSC and HSC to analyse the influence of testing on two different concrete strengths.

Specimen	MCT1	MCT2	MCT3	Specimen	TPB1	TPB2
φ_{cs} (mm)	153	153	153	D (mm)	100	100
φ_{sb} (mm)	8	8	8	B (mm)	100	100
W (mm)	112.5	112.5	112.5	S (mm)	400	400
B (mm)	60	60	60	L (mm)	440	440
e (mm)	4	4	4	a_0 (mm)	5	50
A_{lig} (mm²)	6075	4725	3375	A_{lig} (mm²)	9714	5213

Table 2: Dimensions of MCT and TPB specimens experimentally tested.

To determine the mechanical properties of NSC and HSC the following tests were carried out. The compressive strength is determined from cube specimens of 100 mm side in accordance with UNE EN 12930-3:2009 [8]. The indirect tensile strength is obtained from splitting tests using 100 mm diameter by 200 long cylinders, according to UNE EN 12930-6:2010 [10]. The Young's modulus is determined according to UNE EN 12390-13:2014 [7]. The mechanical properties for NSC

are the following: an average value on compressive strength of 36.8 ± 2% MPa, splitting tensile strength of 3.8 ± 9% MPa and Young's modulus of 24.4 ± 4% GPa and for HSC, compressive strength of 97.0 ± 3% MPa, splitting tensile strength of 5.7 ± 4% MPa and Young's modulus of 41.3 ±3%, detail see in [5].
The experimentally obtained maximum values of load for various notch length are shown in Tab. 3.

Specimen	MCT1	MCT2	MCT3	TPB1	TPB2
α [-]	0.1	0.3	0.5	0.05	0.5
P_{max}, NSC [N]	3667	2956	1168	6329	1987
P_{max}, HSC [N]	7178	3584	2148	9581	3754

Table 3: Crack length ratio for each specimen and experimental values of maximum load on NSC and HSC.

CALIBRATION CURVES FOR MCT

For this work are used the results presented by Seitl and Viszlay [26] for MCT tests through 2D and 3D finite element model of steel bars and cement based materials. In their contribution, four mechanical fracture parameters (stress intensity factor, *T*-stress, crack opening displacement – COD and crack mouth opening displacement – CMOD) are evaluated by means of two finite element models, one of them 2D and the another 3D. All cases (2D and 3D model) were carried out for concrete with five various Young's modulus (E = 5, 20, 25, 60, 100 GPa) and the same Poisson ratio 0.2. The material was assumed to be homogeneous, isotropic with linear elastic behavior. The finite element software ANSYS was used for numerical analysis. For this paper, the calibration curves for E = 40 GPa were calculated. Obtained calibration curves used here for normalized stress intensity factor (B_1) and *T*-stress, as B_2, are follows:

For stress intensity factor, K_I:

$$B_{1\_2D}(E=25,\alpha)=-4.4888+157.35\alpha-992.61\alpha^2+2913.2\alpha^3-3845.6\alpha^4+1937.8\alpha^5 \quad (1)$$

$$B_{1\_2D}(E=40,\alpha)=-12.87+314.45\alpha-1992.3\alpha^2+5711.8\alpha^3-7387.7\alpha^4+3597.5\alpha^5 \quad (2)$$

$$B_{1\_3D}(E=25,\alpha)=-19.17+437.74\alpha-2795.2\alpha^2+7977.5\alpha^3-10259\alpha^4+4936.2\alpha^5 \quad (3)$$

For parameter *T*-stress:

$$B_{2\_2D}(E=25,\alpha)=-0.352+2.6238\alpha+2.2014\alpha^2-9.8235\alpha^3+7.4131\alpha^4 \quad (4)$$

$$B_{2\_2D}(E=40,\alpha)=-0.2776+1.8433\alpha+4.7557\alpha^2-13.039\alpha^3+8.8474\alpha^4 \quad (5)$$

$$B_{2\_3D}(E=25,\alpha)=-0.2905+2.2439\alpha+2.305\alpha^2-8.4968\alpha^3+6.315\alpha^4 \quad (6)$$

Evaluation of measured data

The fracture properties, we focused in the article, are critical values of stress intensity factor and of *T*-stress. The Eqs. (7) and (8) were used to calculate the stress intensity factor and *T*-stress, respectively, for all cases according [16].

$$K_I=\sigma\sqrt{\pi a}B_1 \quad (7)$$

$$T=\frac{K_I B_2}{\sqrt{\pi a}} \quad (8)$$

where a is a crack length, B_1 and B_2 are calibration curves for SIF a T-stress and σ is applied stress for TPB, stress is calculated through following equation, see [28]:

$$\sigma = \frac{3PS}{2BD^2} \tag{9}$$

and for CT and MCT specimen is calculated through following equation, see [16].

$$\sigma = \frac{P}{B\sqrt{W}} \tag{10}$$

For evaluation of measured data, the calibration functions for TPB and CT specimens are well known and are taken from Handbook, e.g. [28], [16].For stress intensity factor and T-stress are follow:

TPB for S/D=4

$$B_1(\alpha) = 0.4487 + 17.782\alpha - 156.01\alpha^2 + 533.83\alpha^3 - 768.03\alpha^4 + 400.1\alpha^5 \tag{11}$$

$$B_2(\alpha) = -0.6016 + 2.2111\alpha - 2.2529\alpha^2 + 0.4647\alpha^3 + 1.7727\alpha^4 \tag{12}$$

and for CT

$$B_1(\alpha) = -2.5552 + 183.27\alpha - 1544.2\alpha^2 + 5315.4\alpha^3 - 7728.2\alpha^4 + 4060.3\alpha^5 \tag{13}$$

$$B_2(\alpha) = 0.5804 - 4.1331\alpha + 18.206\alpha^2 - 28.239\alpha^3 + 15.294\alpha^4 \tag{14}$$

Note that used geometries of measured TPB and MCT specimens are shown in Tab. 2 and their values of maximum loads, P_{max}, can be seen in Tab. 3.
Now, Tab. 4 shows the evaluated data from experimental measurement performed on two kinds of concrete, values of SIF and T-stress for each experiment. Evaluation of MCT data for NSC is done by using tree different calibration curves, the first one for CT specimen Eqs. (13) and (14), second one for MCT2D Eqs. (1) and (4) and MCT3D Eqs. (3) and (6). Evaluation of MCT data for HSC is done by using two different calibration curves, the first one for CT specimen Eqs. (13) and (14) and second one for MCT2D Eqs. (2) and (5).

Calibration function	NSC – K_I [MPa m$^{1/2}$]				HSC – K_I [MPa m$^{1/2}$]			
a	0.05	0.1	0.3	0.5	0.05	0.1	0.3	0.5
CT	-	0.552	0.826	0.560	-	1.080	1.001	1.031
MCT2D	-	0.705	0.872	0.582	-	1.258	0.910	1.193
MCT3D	-	0.666	0.863	0.582	-	-	-	-
TPB	0.472	-	-	0.664	0.710	-	-	1.254
	NSC – T-stress [MPa]				HSC – T-stress [MPa]			
CT	-	1.359	0.695	0.715	-	2.660	0.842	1.315
MCT2D	-	-0.319	1.170	1.034	-	-0.321	1.176	2.185
MCT3D	-	-0.181	1.092	1.025	-	-	-	-
TPB	-1.786	-	-	0.198	-2.700	-	-	0.373

Table 4: Values of stress intensity factor and T-stress versus relative crack length for MCT and TPB specimens made from NSC and HSC. MCT values are evaluated for three different calibration curves CT, MCT2D and MCT3D.

DISCUSSION

Two mixtures of (Normal and High strength) concrete were evaluated from experimental measurement. The experiment was prepared on geometrically different (MCT and TPB) specimens with various initial notch length. Results of NSC stress intensity factor, K_I, for each type of test and relative crack length, α, are shown in Fig. 2. The first row, marked CT, is measured value on modified compact tension specimen but evaluated by using calibration curve for CT (geometry similar), that is very easily find in literature e.g. [2, 16, 22]. The CT values are different from MCT2D and MCT3D values the application of loads on CT and MCT is not exactly equal and consequently stress-field in the material is differently distributed. Therefore, the calibration curves for MCT has to be surely calculated. The values of SIF for MCT2D and MCT3D, for each relative crack length, are very similar and we do not need for evaluation relatively demanding 3D calculation. Note that the TPB test are recommended by RILEM [24] for obtaining fracture properties, in recommendation is written that relative crack length has to be equaled 0.5. Therefore, the obtain values for TPB test is compared with another results.

From literature, the constraint effect is known, especially for metallic materials [19, 20, 25]. Note that for brittle materials, depending on the geometry and loading configurations, the *T*-stress in real engineering components can vary significantly under their service conditions, see in contributions published by Ayatollahi et al. [3] or by Zhao [35] and literature review by Gupta et al. [12].

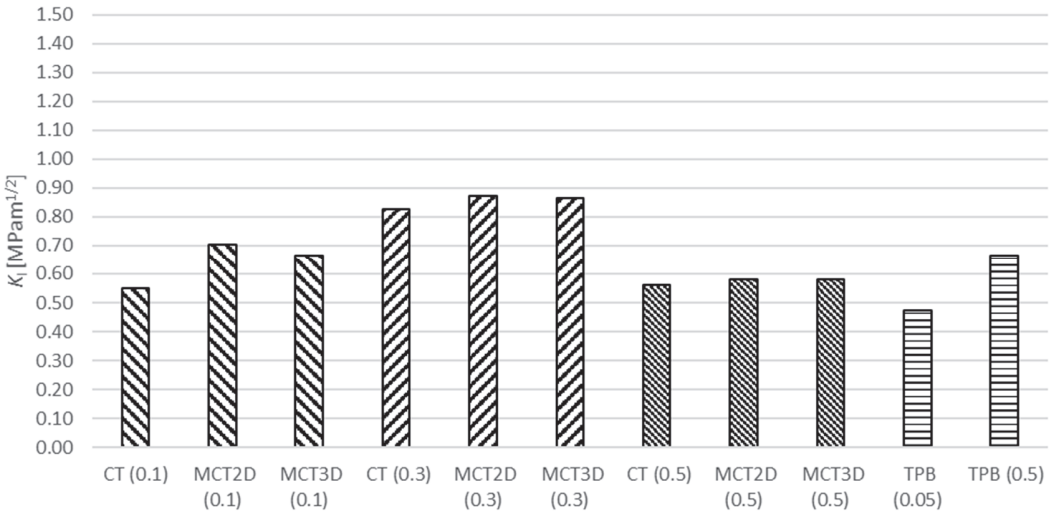

Figure 2: Stress intensity factor, K_I, values for each used procedure and crack length ratio, α, on NSC (E=24.4 GPa).

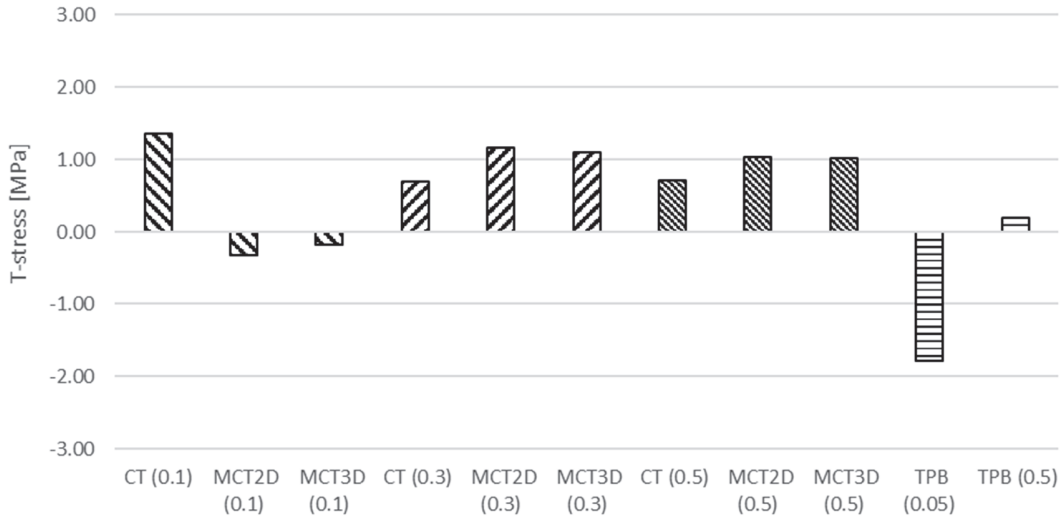

Figure 3: *T*-stress values for each used procedure and crack length ratio, α, on NSC (E=24.4 GPa).

In Fig. 3, it can be seen the results of *T*-stress for each test and relative crack length, α. In this case, there is barely difference on MCT2D and MCT3D results, as it occurs for SIF values. The *T*-stress values are in interval -2 MPa to 2 MPa.
Similar trends are shown in Fig. 4 and 5 for SIF and *T*-stress evaluated for HSC.
The *T*-stress values of HSC for each analyzed test and different relative crack length is shown in Fig. 5. The necessary stress intensity factor values to obtain the *T*-stress are those correspond to Fig. 4 and previously calculated. The results follow a trend like that for NSC, where the main extreme values were achieved for lower relative crack length.
To analyse the influence of both stress intensity factor and *T*-stress parameters in the material, it has been plotted these data for MCT and TPB tests in Fig. 6. T-stress is dimensionless in Fig. 6.a to obtain a trend without variability of this property. Both values are dimensionless to not include the influence of the material in Fig. 6.b.
In Fig. 7.a and b was performed the same analyses for HSC regarding the relation between SIF and *T*-stress, previously carried out for NSC. As it can be seen, both parameters follow a linear tendency, so when the *T*-stress is higher the SIF increases.

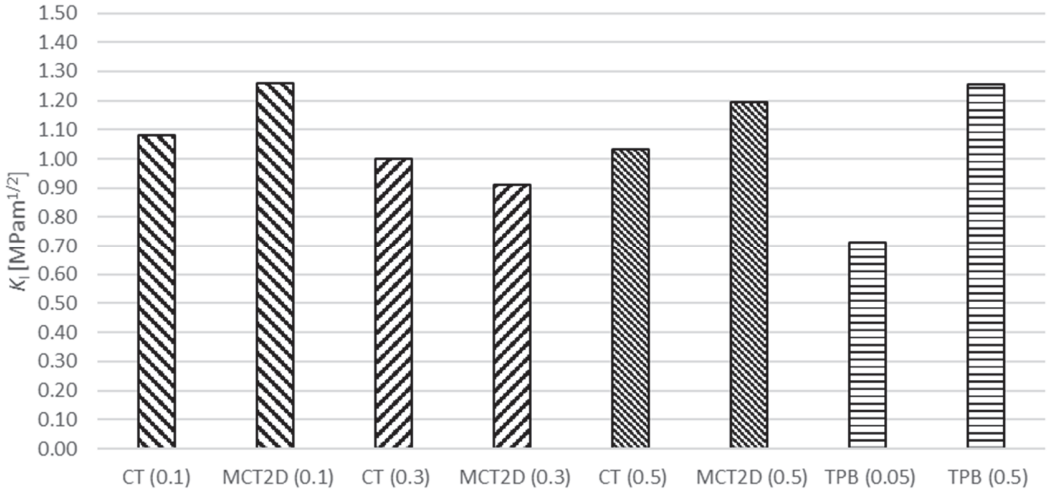

Figure 4: Maximal values of stress intensity factor, K_I, values for each used procedure and crack length ratio, α, on HSC (*E*=41.3 GPa).

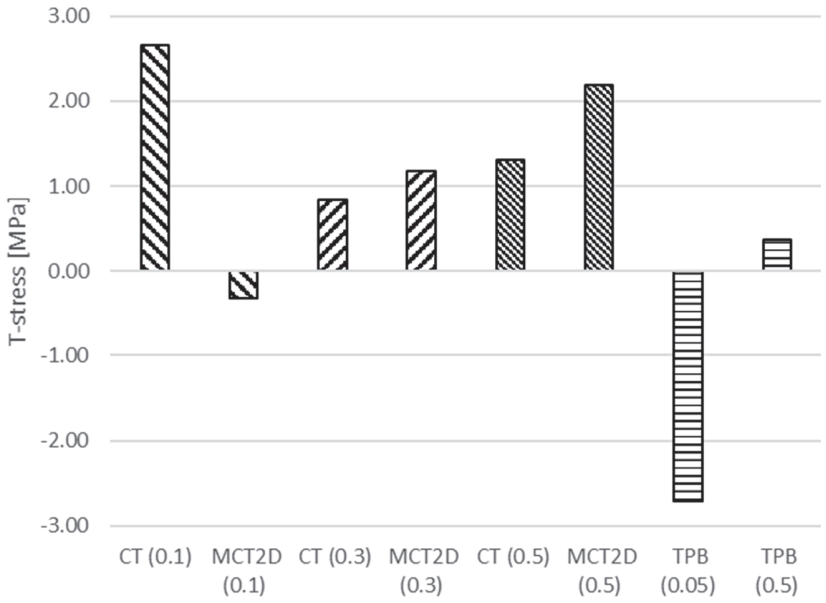

Figure 5: *T*-stress values for each used procedure and crack length ratio, α, on HSC (*E*=41.3 GPa).

There is a slight variation among CT, MCT2D and TPB values. The explanation to these differences were given for NSC. It is worth noticing the remarkable higher values for HSC compared to NSC results.

The tendency line of NSC and HSC, for dimensionless SIF and *T*-stress, are plotted in Fig. 8. As it can be seen the two curves are practically the same, as it can be proved from their linear equation shown in Fig. 8. The coefficient of correlation reveal that the data are significantly scattered because they are used to obtain the linear tendency MCT and TPB tests. In spite of this, the results show reliable and useful behaviour. The dominant role for evaluation of data is played by geometry [35].

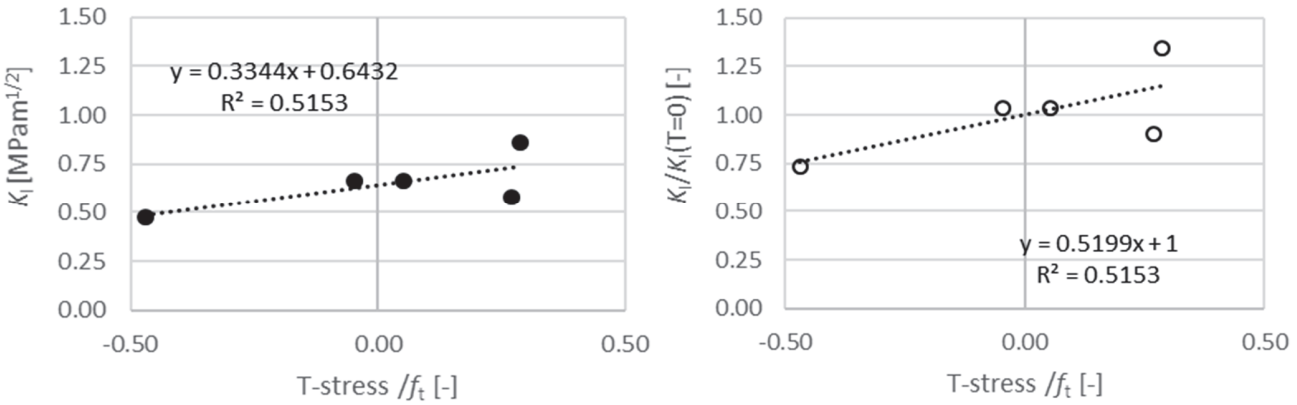

Figure 6: Tendency curve of evolution of *T*-stress/f_t related to K_I on NSC.

The T-stress value for MCT specimen is positive for relative crack length 0.5 and we could recommend this test for obtaining fracture toughness from core drill specimen.

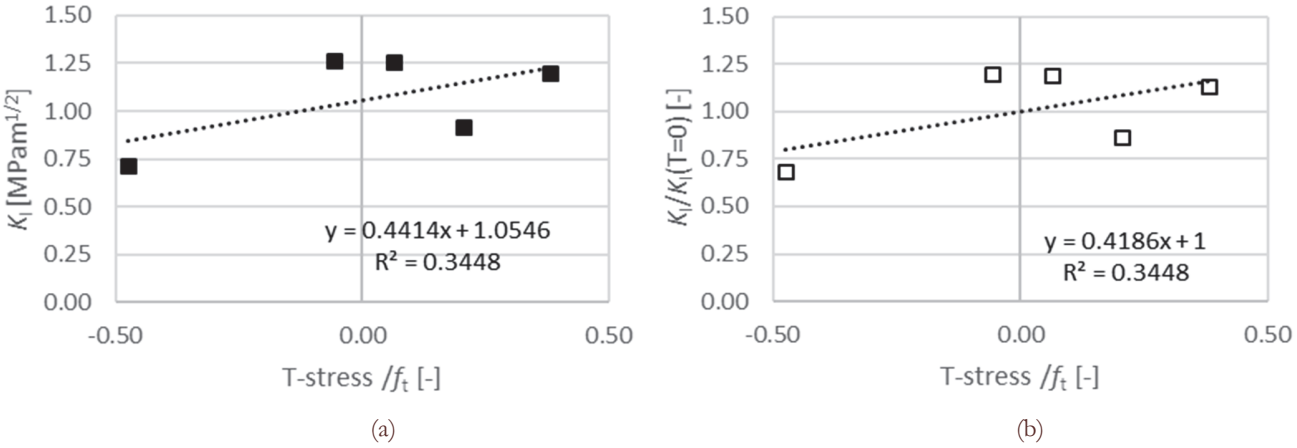

Figure 7: Tendency curve of evolution of *T*-stress/f_t related to K_I on HSC.

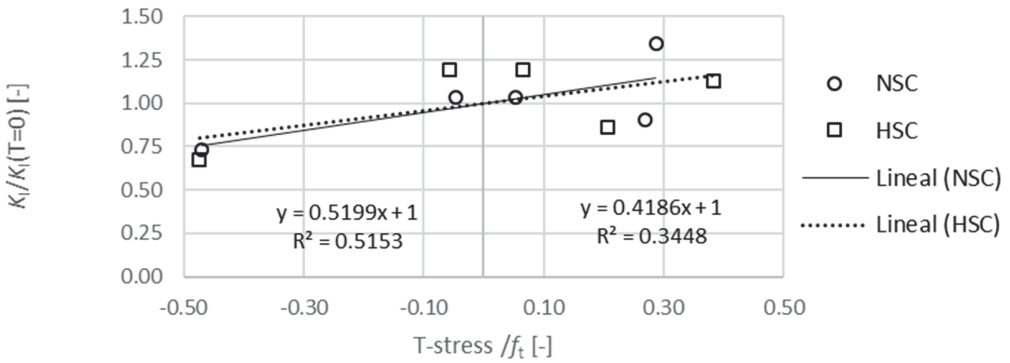

Figure 8: Comparison of tendency curve of evolution of *T*-stress/f_t related to K_I (dimensionless) on NSC and HSC.

Conclusions

The outputs of the experiments have been processed and the values of fracture mechanics parameters (maximal value of stress intensity factor, K_{IC}, and T-stress) have been obtained and discussed using the outputs-calibration curves from previous and newly performed numerical simulations. The following conclusions are drawn:

- Using CT-calibration function leads to not very reliable results compared with calibration functions calculated for MCT2D and MCT3D.
- T-stress results achieved their more extreme values for smaller crack length ratios for any type of test – it is recommended to measured data from relative crack length 0.3.
- For the evaluation of experimentally obtained data, the MCT2D calibration curves can be used instead of MCT3D, because the obtained results by both ways provide reliably similar values and it is save the numerical time.
- Dimensionless SIF and T-stress/f_t follow a remarkable linear trend for NSC and HSC and with similar linear equations, this leads to the geometrical shape of specimen plays dominant role.

The MCT specimen can be recommended as a favourite test sample from core drill to obtain information about concrete fracture toughness by considering the contribution of T-stress.

Acknowledgment

The authors acknowledge the support of Czech Sciences foundation project No. 16-18702S, Ministry of Economy and Competitiveness of Spain BIA2013-48352-P. The research was conducted in the frame of IPMinfra supported through project No. LM2015069 of MEYS.

References

[1] ACI 318-1 Building code requirements for reinforced concrete, American Concrete Institute 20111, Detroit, Michigan, USA.
[2] ASTM E399-90. Standard test method for plane-strain fracture toughness testing of high strength metallic materials. Philadelphia: Amer. Soc. for Testing and Mater; (1990).
[3] Ayatollahi, M.R., Sedighiani, K., A T-stress controlled specimen for mixed mode fracture experiments on brittle materials, European Journal of Mechanics, A/Solids, 36 (2012) 83–93. DOI:10.1016/j.euromechsol.2012.02.008.
[4] Cifuentes, H., Karihaloo, B.L., Determination of size-independent specific fracture energy of normal and high-strength self-compacting concrete from wedge splitting tests, Construction and Building Materials, 48 (2013) 548–553. DOI: 10.1016/j.conbuildmat.2013.07.062.
[5] Cifuentes, H., Lozano, M., Holusova, T., Medina, F., Seitl, S., Canteli, A., Applicability of a modified compact tension specimen for measuring the fracture energy of concrete, Anales de Mecánica de la Fractura, 32 (2015) 208–213.
[6] Cifuentes, H., Lozano, M., Holušová, T., Medina, F., Seitl, S., Fernández-Canteli, A., Modified Disk-Shaped Compact Tension Test for Measuring concrete Fracture Properties, International Journal of Concrete Structures and Materials, (2017). DOI:10.1007/s40069-017-0189-4
[7] EN 12390-13: Testing hardenes concrete – Part 13: Determination of secant modulus of elasticity in compression, AENOR n.d.
[8] EN 12390-3 Testing hardened concrete – Part 3: Compressive strength of test specimens
[9] EN 12390-5 Testing hardened concrete – Part 5: Flexural strength of test specimens
[10] EN12390-6. Testing hardened concrete – Part 6: Tensile splitting strength of test specimens, AENOR n.d.
[11] Guinea, G.V. Elices, M. Planas J., Stress intensity factors for wedge–splitting geometry, Int. J Fracture, 81 (1996) 113–124. DOI: 10.1007/BF00033177.
[12] Gupta, M., Alderliesten, R.C., Benedictus, R., A review of T-stress and its effects in facture mechanics, Engineering Fracture Mechanics, 134 (2015) 218–241. DOI :10.1016/j.tafmec.2015.02.001.
[13] Havlíková, I., Majtánová, R.V., Šimonová, H., Láník, J., Keršner, Z., Evaluation of three-point bending fracture tests of concrete specimens with polypropylene fibres via double-K model, Key Engineering Materials, 592-593 (2014) 185–188. DOI: 10.4028/www.scientific.net/KEM.592-593.185.

[14] Holušová, T., Seitl S., Cifuentes, H., Fernandez-Canteli, A., A numerical study of two different specimen fixtures for the modified compact tension test — their influence on concrete fracture parameters, Frattura ed Integrita Strutturale, 10 (35) (2016) 242–249. DOI: 10.3221/IGF-ESIS.35.28.
[15] Karihaloo, B.L., Fracture Mechanics and Structural Concrete, USA: Longman Scientific and Technical Publishers, (1995) 346.
[16] Knésl, Z. Bednář, K., Two–parameter fracture mechanics: Calculation of parameters and their values, Institute of Physics of Materials Academy of Science of the Czech Republic, (1998).
[17] Korte, S., Boel, V., De Corte, W., De Schutter, G., Static and fatigue fracture mechanics properties of self–compacting concrete using three–point bending tests and wedge–splitting tests. Construction and Building Materials, 57 (2014) 1–8. DOI: 10.1016/j.conbuildmat.2014.01.090
[18] Linsbauer, H.N., Tschegg, E.K, Fracture energy determination of concrete with cube shaped specimens, Zement und Beton, 31 (1986) 38–40.
[19] Matvienko, Y.G., Two approaches to taking nonsingular T-stress into account in the criteria of fracture mechanics for bodies with notches, Journal of Machinery Manufacture and Reliability 40(5) (2011) 494–498. DOI: 10.3103/S105261881104011X.
[20] Matvienko, Y.G., Two-parameter fracture mechanics in contemporary strength problems, Journal of Machinery Manufacture and Reliability, 42(5) (2013) 374–381. DOI: 10.3103/S1052618813050087.
[21] Merta, I., Tschegg, E.K., Fracture energy of natural fibre reinforced concrete, Construction and Buildings Materials 40 (2013) 991–997. DOI: 10.1016/j.conbuildmat.2012.11.060.
[22] Murakami, Y., Stress Intensity Factors Handbook, Elmsford NY (USA) Pergamon Books, (1987) 1566.
[23] Pinho, S.T., Robinson, P. Iannucci, L., Fracture toughness of the tensile and compressive fibre failure modes in laminated composites. Composites Science and Technology, 66(13) (2006) 2069–2079.
[24] RILEM 106, Determination of the fracture energy of mortar and concrete by means of three-point bend tests on notched beams, (1985) 285–290.
[25] Seitl, S., Hutař, P., Fatigue crack propagation near threshold region in framework two-parameter fracture mechanics, Journal Materials and Technology, 41(3) (2007) 135–138.
[26] Seitl, S., Viszlay, V., Modified Compact Tension Specimen for Experiments on Cement Based Materials: Comparison of Calibration Curves from 2D and 3D Numerical Solutions. Frattura ed Integrità Strutturale, 39 (2017) 118–128. DOI: 10.3221/IGF-ESIS.39.13.
[27] Seitl, S., Viszlay, V., Cifuentes, H., Fernández-Canteli, A., Effects of specimen size and crack depth ratio on calibration curves for modified compact tension specimens, Transactions of the VŠB –Technical University of Ostrava, Civil Engineering Series, 15(2) (2015) 23. DOI: 10.1515/tvsb-2015-0023.
[28] Tada, H., Paris, P.C., Irwin, G.R., The stress analysis of crack handbook, third ed., The American Society of Mechanical Engineers Three Park Avenue, New York, (2000).
[29] Veselý, V. Frantík, P. Sobek, J., Malíková, L. Seitl, S., Multi-parameter crack tip stress state description for evaluation of nonlinear zone width in silicate composite specimens in component splitting/bending test geometry, Fatigue and Fracture of Engineering Materials and Structures, 38(2) (2015) 200–214. DOI: 10.1111/ffe.12170.
[30] Veselý, V., Merta, I., Šimonová, H., Schneemayer, A., Seitl, S., Keršner, Z., Component wedge-splitting/bending test of notched specimens with various crack-tip constraint conditions: Experiments and simulations, 9th International Conference on Fracture Mechanics of Concrete Structures FraMCoS-9, (2016) 1–12. DOI: 10.21012/FC9.086.
[31] Veselý, V., Sobek, J., Frantík, P., Štafa, M., Šestáková, L., Seitl, S., Estimation of the zone of failure extent in quasi-brittle specimens with different crack-tip constraint conditions from stress field, Key Engineering Materials, 592-593 (2014) 262–265. DOI: 10.4028/www.scientific.net/KEM.592-593.262.
[32] Wagnoner, M.P., Buttlar, W.G., Paulino, G.H., Disk-shaped compact tension test for asphalt concrete fracture, Experimental Mechanics, 45(3) (2005) 270–277 .
[33] Wang, Y., Hu, X.. Liang, L., Zhu, W., Determination of tensile strength and fracture toughness of concrete using notched 3-p-b specimens, Engineering Fracture Mechanics 160 (2016) 67–77. DOI: 10.1016/j.engfracmech.2016.03.036
[34] Williams, M.L., On the stress distribution at the base of stationary crack, ASME Journal of Applied Mechanics, 24 (1957) 109–114.
[35] Zhao, Y. Xu, B., Effect of T-stress on the mode-I fracture toughness of concrete, C. R. Mecanique 342 (2014) 490–500. DOI: 10.1016/j.crme.2014.03.001.